

POST-PROCESSING OF ADDITIVELY MANUFACTURED PURE COPPER RFQ ELEMENTS*

T. Romano[†], M. Vedani, Politecnico di Milano, Milan, Italy

T. Torims, M. Vretenar, CERN, Geneva, Switzerland

C. A. Bloem Irazabal, L. Portolés Griñán, T. M. Zanello Rial, AIDIMME, Valencia, Spain

G. Pikurs, A. Ratkus, Riga Technical University, Riga, Latvia

M. Pozzi, Rösler Italiana S.R.L., Concorezzo, Italy

Abstract

The utmost design freedom of additive manufacturing (AM) can be leveraged to fabricate complex particle accelerator components, such as radiofrequency quadrupoles (RFQs). However, the high surface roughness typical of as-printed parts represents a major barrier to the integration of AM technologies into established fabrication workflows. This work investigates finishing processes aimed at improving the surface quality of additively manufactured RFQ components, with a focus on the hard-to-access vane tip region. A dedicated mock-up was developed, consisting of a copper vane representing a one-quarter RFQ section, mounted in a plastic holder to replicate the full part. This setup allows the copper part to be removed after each treatment step to measure material removal and assess effects on vane modulation and surface roughness. Both mechanical mass finishing with abrasive media and chemical polishing were examined, applying each treatment in multiple intermediate steps. Comprehensive surface characterization was conducted by means of profilometry and roughness measurements, showing that both treatments reduce the roughness primarily through the removal of surface asperities. The mechanical treatment approached a plateau after two cycles, achieving a final Ra of $\sim 4.9 \mu\text{m}$, while the chemical process reached a slightly higher Ra ($\sim 7 \mu\text{m}$) due to material oxidation and partial exhaustion of the solution. Localized peak flattening and deviations in the vane modulation profile indicate the need for further optimization of both design compensation strategies and post-processing conditions.

INTRODUCTION

AM, particularly laser powder bed fusion (LPBF), offers great potential for the fabrication of complex accelerator components, such as RFQs [1], owing to its high design flexibility and its ability to guarantee properties comparable to those of conventionally processed materials [2]. However, the relatively high surface roughness of LPBF-fabricated parts remains a major limitation, as surface irregularities may compromise the breakdown performance and vacuum compatibility of components [3]. For RFQ applications, a Ra of $\sim 0.4 \mu\text{m}$ is typically required [4], making post-processing an essential step.

* This work was carried out as part of the IFAST project within the framework of the European Union's Horizon 2020 Research and Innovation programme under Grant Agreement No. 101004730 and was supported by the Latvian Council of Science under Grant Agreement VPP-IZM-CERN-2022/1-0001.

[†]tobia.romano@cern.ch

In this study, mechanical mass finishing and chemical polishing were investigated as post-processing techniques to improve the surface quality of pure copper RFQ elements manufactured via LPBF, with particular attention to the hard-to-access vane tip region.

MATERIALS AND METHODS

The RFQ samples were fabricated using a TruPrint1000 Green Edition LPBF system equipped with a disk green laser ($\lambda = 515 \text{ nm}$). A linear energy density of 0.625 J/mm was employed to process a 99.95% Cu powder with 15–45 μm particle size, deposited in layers of 40 μm thickness. After printing, the samples were subjected to light blasting using AMACAST 10 stainless steel media. The sample geometry was designed to reproduce one quarter of the CERN 750 MHz RFQ module, as described in [4]. Based on previous measurements conducted on a full RFQ prototype made by LPBF [5], a 250 μm thick allowance was added to the nominal model to compensate for material removal during post-processing. A plastic holder made of polyamide-12 was produced by fused filament fabrication to replicate the full RFQ structure (120 mm in diameter and 150 mm in length) when inserting the copper vane, as shown in Fig. 1.

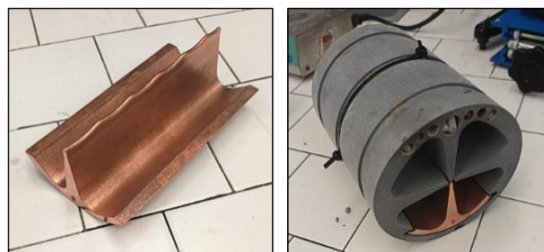


Figure 1: RFQ $\frac{1}{4}$ vane fabricated by LPBF and inserted in plastic holder for post-processing experiments.

Mechanical mass finishing and chemical polishing post-processing routes were investigated. The mechanical treatment consisted of four cycles of 1 h each, performed in a BRS 22 vibratory tumbler with R.Ecoshape 06/10 ZS abrasive media and water. The chemical treatment also included four cycles, each comprising 30 min of immersion in a chemical solution followed by 30 min rinsing. After these steps, two additional vibrofinishing cycles of 4 h were carried out using a R 150 DL tumbler, with the samples in fixed position, and R.Ecoshape 10/20 DZS abrasive media. All equipment and media were developed and supplied by Rösler Italiana. After each step, the samples were extracted from the holder, rinsed with water, and subjected to comprehensive surface characterization by means of

profilometry and roughness measurements. A reference as-blasted sample was also characterized for comparison.

RESULTS AND DISCUSSION

Surface Morphology

Figure 2 shows the vane tip surface morphology at the profile peaks of the samples subjected to mechanical and chemical treatments. A marked flattening effect can be observed in the peak regions after four mechanical cycles (Fig. 2a). This localized flattening can be attributed to fragments of abrasive media that remained trapped within the bore of the assembly during the treatment. A similar effect was also observed in the sample subjected to chemical treatment (Fig. 2b), which also involved rinsing with water and R.Ecoshape 06/10 ZS abrasive media.

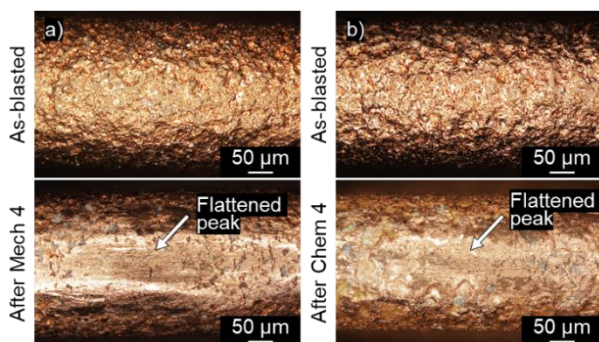


Figure 2: Vane tip surface morphology at profile peak regions of samples subjected to mechanical (a) and chemical treatment (b).

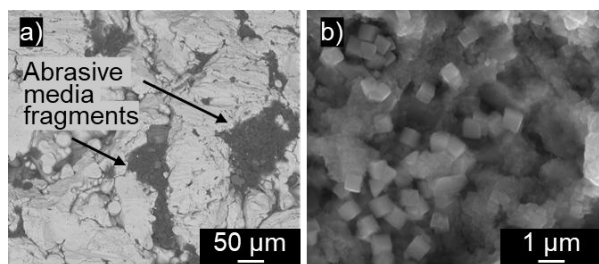


Figure 3: Abrasive media fragments (a) and cubic oxide nanoparticles observed on the surface of samples subjected to mechanical (a) and chemical treatments (b).

In both samples, the mechanical action of the abrasive media removed the peaks of the initial rough surface layer, while valleys are still present. This suggests that larger material removal would be needed to completely eliminate these defects. In the mechanically treated sample, fragments of abrasive media were observed inside the surface cavities (Fig. 3a), as evidenced by the high C and Si contents locally detected by energy dispersive spectroscopy (EDS), primarily attributed to the polymeric matrix and the abrasive SiO₂ component of the media, respectively. Nanometric cubic oxide particles were observed on localized areas of the chemically treated sample, as shown in Fig. 3b. Their formation can be attributed to oxidation caused by prolonged immersion of the part in the solution, with the cubic morphology promoted by the presence of chloride ions in the solution [6].

Material Removal and Tip Thickness

The mechanical treatment did not result in any measurable mass loss and caused only a limited reduction in the tip thickness ($\sim 50 \mu\text{m}$), as the tip area was difficult for abrasive media to reach. The two vibrofinishing cycles produced a comparable overall material removal ($\sim 3.8 \text{ g}$ in the first step and $\sim 3.2 \text{ g}$ in the second). However, the first cycle resulted in a greater reduction in tip thickness ($\sim 100 \mu\text{m}$), suggesting that during the second cycle ($\sim 30 \mu\text{m}$ reduction) material was removed mainly from sample regions that were more easily accessible to the abrasive media.

The chemical treatment exhibited a much higher material removal rate, with a mass loss of 6–8 g after each cycle, attributable to the action of the chemical solution. A substantial reduction in tip thickness ($\sim 120 \mu\text{m}$) was observed after the first step, due to the extensive removal of the oxide layer initially present on the part surface. Subsequent cycles resulted in limited reductions of $\sim 20\text{--}30 \mu\text{m}$. The first vibrofinishing cycle had a strong effect on both mass loss ($\sim 5.5 \text{ g}$) and tip thickness reduction ($\sim 180 \mu\text{m}$), which can be attributed to the partial removal of surface oxides formed during prolonged immersion in the chemical solution. The second cycle had a moderate effect ($\sim 1 \text{ g}$ mass loss and $\sim 20 \mu\text{m}$ tip thickness reduction).

Tip Profile

Table 1: Tip Profile Parameters of Samples Subjected to Mechanical (Mech) and Chemical (Chem) Treatments

Sample	Cycle	Ampl. [mm]	Peak distance [mm]		
			1 st -2 nd	2 nd -3 rd	3 rd -4 th
Model	Nom.	1.80	26.72	26.49	25.68
	Blasted	1.81	26.51	25.80	25.77
	Mech	Mech 4	1.78	26.26	26.20
Mech	Vibro 2	1.75	26.52	26.22	25.29
	Blasted	1.82	26.61	25.57	25.76
	Chem	Chem 4	1.76	26.43	25.56
Chem	Vibro 2	1.76	26.38	25.68	25.75

Table 1 reports the main profile parameters of the samples subjected to post-processing experiments. The mechanically treated sample shows a $\sim 0.2 \text{ mm}$ lower amplitude compared to the nominal value after mechanical cycles and $\sim 0.5 \text{ mm}$ lower after the vibrofinishing steps. In the chemically treated sample, this difference is $\sim 0.4 \text{ mm}$ after chemical cycles and remains unchanged after vibrofinishing. This can be primarily attributed to localized flattening at the peak regions of post-processed samples, indicating the need for more accurate compensation during the design stage.

Regarding peak spacing, the mechanically treated sample shows a $\sim 0.2\text{--}0.4 \text{ mm}$ mismatch compared to the nominal geometry, while still maintaining the decreasing trend in peak spacing required for RFQ functionality. The chemically treated sample exhibits a discrepancy of $\sim 0.3\text{--}0.8$

mm, without a clear decreasing trend in peak spacing. More precise measurements, possibly using 3D scanning, and greater geometric accuracy of the tip profile will be performed to meet design specifications.

Surface Roughness

The surface roughness parameters of the investigated samples in the various conditions are shown in Fig. 4. For the mechanically treated part, roughness parameters show a clear decreasing trend up to the second cycle (Fig. 4a). A similar behavior is observed for the peak-related parameters (R_p , R_z , R_t), indicating an effective removal of the highest asperities. The last two cycles led to moderate decrease in roughness, suggesting that the process approaches a plateau. Overall, R_a decreased from $12.5 \mu\text{m}$ to $5.3 \mu\text{m}$ after four mechanical cycles. A similar trend is observed for R_q ; however, the R_q/R_a ratio slightly increased from ~ 1.25 to ~ 1.35 during the treatment, which may be attributed to the remaining deeper valleys that were not effectively removed by the process, as also suggested by the limited decrease in R_v . Vibrofinishing had an additional smoothing effect, resulting in a final R_a of $\sim 4.9 \mu\text{m}$.

The chemical treatment led to a decrease in roughness parameters up to cycle 3 (R_a decreases from ~ 11 to $\sim 7 \mu\text{m}$), followed by an increase during cycle 4 (R_a of ~ 8.9) due to part oxidation caused by prolonged immersion in the chemical solution, localized surface effects associated with the chemical process, and reduced smoothing efficiency due to partial exhaustion of the chemical agents. Roughness slightly decreased after vibrofinishing, resulting in a final R_a of $\sim 7.7 \mu\text{m}$, possibly due to partial removal of surface oxides, which were only observed in localized regions during SEM analyses.

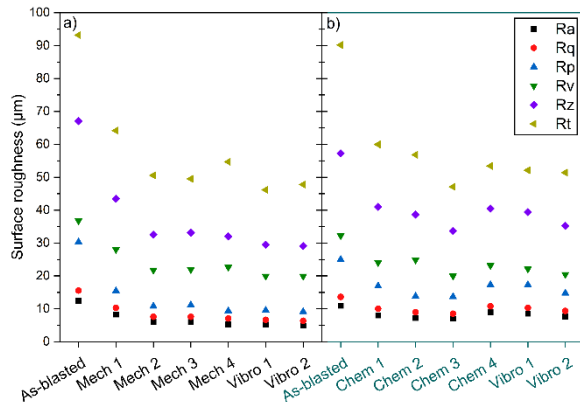


Figure 4: Surface roughness of samples subjected to mechanical (a) and chemical treatments (b).

Figure 5 shows the 3D roughness maps of the samples in as-blasted condition and after four mechanical and chemical cycles. Consistent with 2D roughness data, the mechanical treatment reduced S_a from ~ 20.3 to $\sim 11.6 \mu\text{m}$. However, S_{sk} became more negative (from -0.4 to -2.1), indicating a predominance of valleys over peaks as a result of the abrasion process. This is also reflected in the strong reduction of S_p (from ~ 109.2 to $\sim 27.6 \mu\text{m}$), while S_v remained relatively high ($\sim 156.3 \mu\text{m}$ in as-blasted condition and $\sim 141.4 \mu\text{m}$ after the mechanical treatment).

The chemical process resulted in only minor changes in the average surface parameters (with S_a values of $\sim 16.9 \mu\text{m}$ in as-blasted condition and $\sim 17.3 \mu\text{m}$ for the treated sample), likely due to the increase in surface roughness following the last cycle, as also indicated by the 2D roughness data. However, S_p decreased from ~ 84.4 to $\sim 51.0 \mu\text{m}$, suggesting significant removal of surface peaks during the mechanical part of the treatment. Compared to the purely mechanical process, S_v was reduced to a higher extent (from ~ 137.3 to $\sim 109.6 \mu\text{m}$), indicating a more uniform material removal due to the action of the chemical solution.

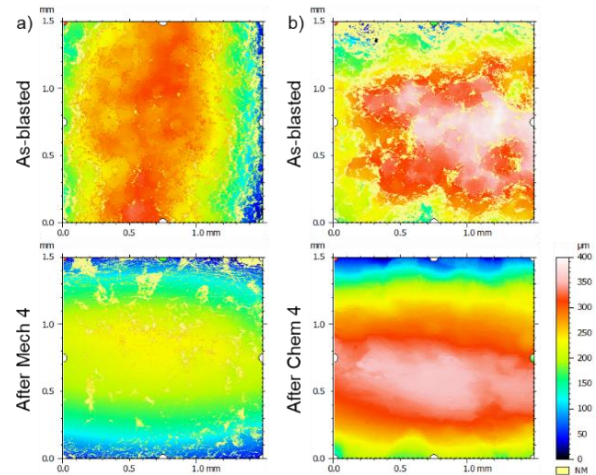


Figure 5: 3D roughness maps of samples subjected to mechanical (a) and chemical treatments (b).

CONCLUSIONS

This study investigated mechanical and chemical post-processing to improve the surface finishing of copper RFQ components fabricated by LPBF. A removable one-quarter RFQ mock-up, mounted in a dedicated plastic holder replicating the full bore, enabled systematic monitoring of material removal, surface roughness evolution, and tip-profile modifications throughout successive finishing cycles. Mechanical finishing provided the largest roughness reduction during the first two cycles, reaching a plateau at a final R_a of $\sim 4.9 \mu\text{m}$. Chemical polishing remained effective up to the third cycle, yielding a R_a of $\sim 7 \mu\text{m}$, followed by a slight roughness increase due to oxidation and partial chemical agent depletion. Hence, the obtained R_a values remained considerably higher than the target of $\sim 0.4 \mu\text{m}$. Localized peak flattening due to trapped abrasive media fragments and discrepancies between nominal and measured peak-spacing trends also revealed limitations in material removal uniformity and geometric preservation. Therefore, the investigated procedures cannot yet be considered fully validated finishing routes for operational RFQs. However, the results identify key challenges in post-processing of AM-fabricated RFQs, including the limited roughness reduction achievable with the investigated mechanical and chemical methods and the susceptibility of complex RFQ geometries to non-uniform material removal. Further development of treatment parameters and monitoring will be needed to achieve the required surface quality, including multiple sample testing to assess process repeatability.

REFERENCES

- [1] T. Torims *et al.*, “Evaluation of geometrical precision and surface roughness quality for the additively manufactured radio frequency quadrupole prototype”, *J. Phys. Conf. Ser.*, vol. 2420, vol. 1, pp. 012089, 2023.
[doi:10.1088/1742-6596/2420/1/012089](https://doi.org/10.1088/1742-6596/2420/1/012089)
- [2] T. DebRoy *et al.*, “Additive manufacturing of metallic components – Process, structure and properties”, *Prog. Mater. Sci.*, vol. 92, pp. 112-224, 2023.
[doi:10.1016/j.pmatsci.2017.10.001](https://doi.org/10.1016/j.pmatsci.2017.10.001)
- [3] T. Romano *et al.*, “Metal additive manufacturing for particle accelerator applications”, *Phys. Rev. Accel. Beams*, vol. 27, pp. 054801, 2024.
[doi:10.1103/PhysRevAccelBeams.27.054801](https://doi.org/10.1103/PhysRevAccelBeams.27.054801)
- [4] T. Torims *et al.*, “First proof-of-concept prototype of an additively manufactured radio frequency quadrupole”, in *Instruments*, vol. 5, no. 4, pp. 35,
[doi:10.3390/instruments5040035](https://doi.org/10.3390/instruments5040035)
- [5] T. Torims *et al.*, “Development of additively manufactured 750 MHz RFQ”, in *Proc. LINAC'24*, Chicago, USA, August 2024, pp. 600-6003.
[doi:10.18429/JACoW-LINAC2024-THAA003](https://doi.org/10.18429/JACoW-LINAC2024-THAA003)
- [6] M.H. Kim *et al.*, “Polyol synthesis of Cu₂O nanoparticles: Use of chloride to promote the formation of a cubic morphology”, in *J. Mater. Chem.*, Vol. 18, no. 34, pp. 4069-4073.
[doi:10.1039/b805913f](https://doi.org/10.1039/b805913f)